Ain Shams Engineering Journal (2015) xxx, xxx–xxx

Ain Shams University

Ain Shams Engineering Journal

www.elsevier.com/locate/asej
www.sciencedirect.com

ELECTRICAL ENGINEERING

Load frequency control problem in interconnected power systems using robust fractional PI$^{\lambda}$D controller

Abdelmoumène Delassi *, **Salem Arif** [1], **Lakhdar Mokrani** [2]

Laboratoire d'Analyse et de Commande des Systèmes d'Energie et Réseaux Electriques, Université Amar Telidji de Laghouat, BP 37G, Laghouat 03000, Algeria

Received 2 May 2015; revised 16 September 2015; accepted 14 October 2015

KEYWORDS

Load frequency control;
Fractional controller;
Differential Evolution Algorithm;
Nonlinearities;
Integral of Squared Error

Abstract In this paper, a robust Fractional Order **PI$^{\lambda}$D** controller that contains an integral fraction action and a simple filtered derivative action, is investigated on Automatic Generation Control (AGC) of a three areas reheat-thermal system. For more realistic study some nonlinear constraints have been introduced such as Governor Dead Band (GDB), Generation Rate Constraints (GRC) and boiler dynamics. The optimal controller parameters are tuned through new evolutionary algorithm known as Differential Evolution (DE) algorithm by minimizing the Integral of Squared Error (ISE) index. Obtained results reveal clearly the superiority of the investigated controller compared to the other controllers such as PID, PID$^{\mu}$ and PI$^{\lambda}$D$^{\mu}$ in terms of the performance index, peak overshoots, peak undershoots and settling time. Effectiveness and rapidity of the DE algorithm in the convergence have been shown and compared to Genetic Algorithm (GA). Finally, robustness analysis against higher degree of load disturbance and sever parametric variation demonstrates the effectiveness of the investigated controller.

1. Introduction

The main objective of an electrical power system is to ensure the balance between the total power generation with the total load demand and the associated system losses, then regulating the system frequency and tie-line power exchange [1,2]. To ensure the quality of power supply, it is obligatory to regulate the generator loads depending on the optimal frequency value through a secondary controller [3]. This scheme is known as the Load Frequency Control (LFC), named also AGC. It is one of the most important control problems in the design and operation of power systems, whose role is [4–7]: to keep

* Corresponding author. Tel.: +213 798 74 92 15.
E-mail addresses: a.delassi@lagh-univ.dz (A. Delassi), s.arif@lagh-univ.dz (S. Arif), l.mokrani@mail.lagh-univ.dz (L. Mokrani).
[1] Tel.: +213 662 16 25 88.
[2] Tel.: +213 773 93 26 27.

Peer review under responsibility of Ain Shams University.

ELSEVIER Production and hosting by Elsevier

http://dx.doi.org/10.1016/j.asej.2015.10.004
2090-4479 © 2015 Faculty of Engineering, Ain Shams University. Production and hosting by Elsevier B.V.

Nomenclature

PID	Proportional Integral Derivative
FO-PID	Fractional Order Proportional Integral Derivative
LFC	Load Frequency Control
AGC	Automatic Generation Control
ACE	Area Control Error
GRC	Generation Rate Constraint
GDB	Governor Dead Band
DE	Differential Evolution
ISE	Integral of Squared Error
Δf_i	frequency deviation of area i (Hz)
ΔP_{m1}	mechanical power deviation for the area i (pu)
ΔP_{Ci}	power deviation of area i
ΔP_{Li}	load variation of area i
T_{Gi}	steam turbine speed governor time constant (s)
K_{Ri}	coefficient of reheater steam turbine
T_{Ri}	reheater time constant (s)
T_{Ti}	steam turbine time constant (s)
K_{Pi}	power system gain constant
T_{Pi}	power system time constant (s)
R_i	speed regulation value (Hz/p.u)

the frequency unchanged by the load, to keep the correct value of interchanged power between control areas, to maintain each unit's generation at the most economic value and the last objective is to ensure the non-violation of operating limits.

Different control strategies have been proposed in the literature for this secondary controller design. The most widely used are the classical PI and PID controllers [8–10] due to their implementation simplicity. The synthesis of these controllers is based on the power system model. Hence, a variation of the model parameters or the system operating points leads to the degradation of the controlled system performances. To rectify these problems, other emerging strategies have been proposed to enhance the performance of such classical controllers.

Some researchers proposed the use of two degrees of freedom PID controller in two and three areas considering some nonlinear constraints such as GDB and GRC [11,19]. Other propositions based on fuzzy logic controller have been proposed in two area reheat-thermal systems taken into account GDB and GRC constraints [12]. The use of fractional controller has been also implemented by several researchers [13,14,17,18]. In [17], the authors have proposed $I^{\lambda}D^{\mu}$ controller in three areas reheat-thermal AGC system with consideration of GRC. Authors in [18] proposed two-degrees of freedom PID (2-DOF-PID) controller in three areas reheat-thermal system with GRC constraints.

Owing to the complexity of the system, direct synthesis of the above proposed controllers is not straightforward. Therefore, an optimization of the controller parameters based on different techniques appears to be an attractive solution. The optimization techniques extensively used in the AGC problem are as follows: GA, Particle Swarm Optimization (PSO), Bacterial Foraging Optimization Algorithm (BFOA) and hybridization of PSO–BFOA [8–11,15].

In this paper, an attempt has been made for the optimal fractional **$PI^{\lambda}D$** controller design, made up with a fractional integral action and a simple filtered derivative action and applied to a three areas reheat-thermal AGC systems considering several nonlinearity constraints. The investigated controller will provide more effective compared to the simple PID controller and a fractional PID controllers such as PID^{μ} and $PI^{\lambda}D^{\mu}$ from different points of view. The design problem is formulated as an optimization problem in the basis of evaluating the ISE criterion. Then, the DE algorithm has been used to determine the optimal controller parameters. Simulation results show the effectiveness of the investigated controller in terms of performances index; and its robustness against a wide range of loading conditions, disturbance and parametric variation. Furthermore, the superiority of the investigated optimization algorithm is illustrated via a comparison with other evolutionary algorithm, which is the GA. In view of the above presentation, the main goals of this work are as follows:

- To design a robust fractional **$PI^{\lambda}D$** controller and compare its performance with others known controllers as well as; PID, PID^{μ} and $PI^{\lambda}D^{\mu}$ in a three areas reheat-thermal system with consideration of GDB, GRC and dynamic boiler.
- To optimize the above mentioned controllers using DE algorithm and compare its convergence characteristics with GA.
- To verify the robustness of obtained optimal value of the investigated (**$PI^{\lambda}D$**) controller through different load disturbance and sensitivity analysis.

2. Power system modeling

The investigated **$PI^{\lambda}D$** controller is tested on three areas interconnected reheat-thermal AGC system as shown in Fig. 1 [16]. For more realistic analysis, some nonlinear constraints such as GDB, GRC and dynamic boiler are taken into account [11].

The transfer function model of the system under study is depicted in Fig. 2. The dynamic boiler scheme is presented in Appendix B. The nominal system parameters [17–19] are recapitulated in Appendix A. A dynamical frequency responses of the first area (Δf_1) with and without nonlinearities are presented in Fig. 3.

From Fig. 3, it has been noted that the system without any control is stable but it represents a steady state error. Hence, to reduce this error, we have implemented (**$PI^{\lambda}D$**) controller.

3. Fractional calculus background

In mathematics, fractional calculus permits to convert the differential or integral operator with integer order to the fractional order [13]. The fractional operator noted ${}_aD_t^{\alpha}$, depending on the sign of α indicates differentiation or integration. This operator is presented in Eq. (1). There are some existing definitions for describing the fractional order functions. The most frequently used are, Riemann–Liouville

Please cite this article in press as: Delassi A et al., Load frequency control problem in interconnected power systems using robust fractional $PI^{\lambda}D$ controller, Ain Shams Eng J (2015), http://dx.doi.org/10.1016/j.asej.2015.10.004

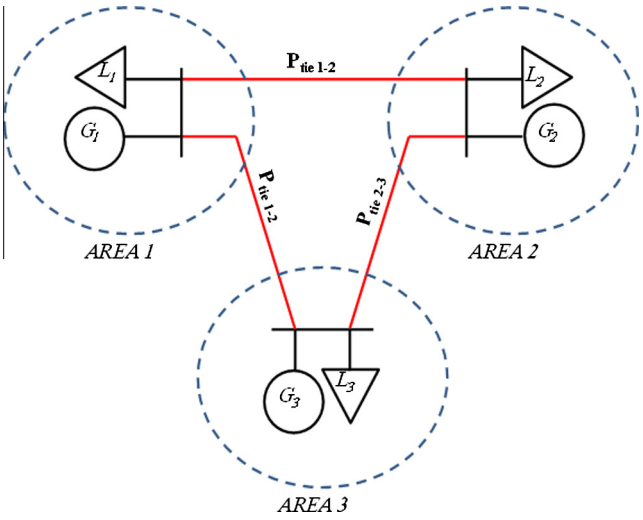

Figure 1 Three areas AGC systems.

definition given by Eq. (2), Grünwald–Ltnikov definition given by Eq. (3) and Caputo definition given by Eq. (4).

$$\begin{cases} d^{\alpha}/dt^{\alpha}, & \alpha > 0 \\ 1, & \alpha = 0 \\ \int_0^t (d\tau)^{\alpha}, & \alpha < 0 \end{cases} \tag{1}$$

$${}_aD_t^{\alpha} f(t) = \frac{1}{\Gamma(n-\alpha)} \frac{d^n}{dt^n} \int_{\alpha}^{t} \frac{f(\tau)}{(t-\tau)^{1-(n-\alpha)}} d\tau \tag{2}$$

$${}_aD_t^{\alpha} f(t) = \lim_{h \to 0} \frac{1}{\Gamma(\alpha) h^{\alpha}} \sum_{k=0}^{[(t-a)/h]} \frac{\Gamma(\alpha+k)}{\Gamma(k+1)} f(t-kh) \tag{3}$$

$${}_0D_t^{\alpha} f(t) = \frac{1}{\Gamma(m-\alpha)} \int_0^t \frac{f^{(m)}(\tau)}{(t-\tau)^{\alpha-m+1}} d\tau \tag{4}$$

To implement the fractional controller in simulation studies or in practice, one method is to approximate them with integer order transfer functions [20]. Practically, five continuous approximations are available such as Crone approximation, Carlson approximation, Matsuda approximation, the high-frequency continued fraction approximation and the low-frequency continued fraction approximation. Crone (French acronym of commande robust d'ordre non entier) approximation is adopted in this study. This approximation uses a recursive distribution of N poles and N zeros leading to the following transfer function [21]:

$$C(s) = K' \prod_{n=1}^{N} \frac{1 + (s/\omega_{zn})}{1 + (s/\omega_{pn})} \tag{5}$$

where K' is an adjusted static gain. Zeros and poles are determined inside a frequency range and are given below:

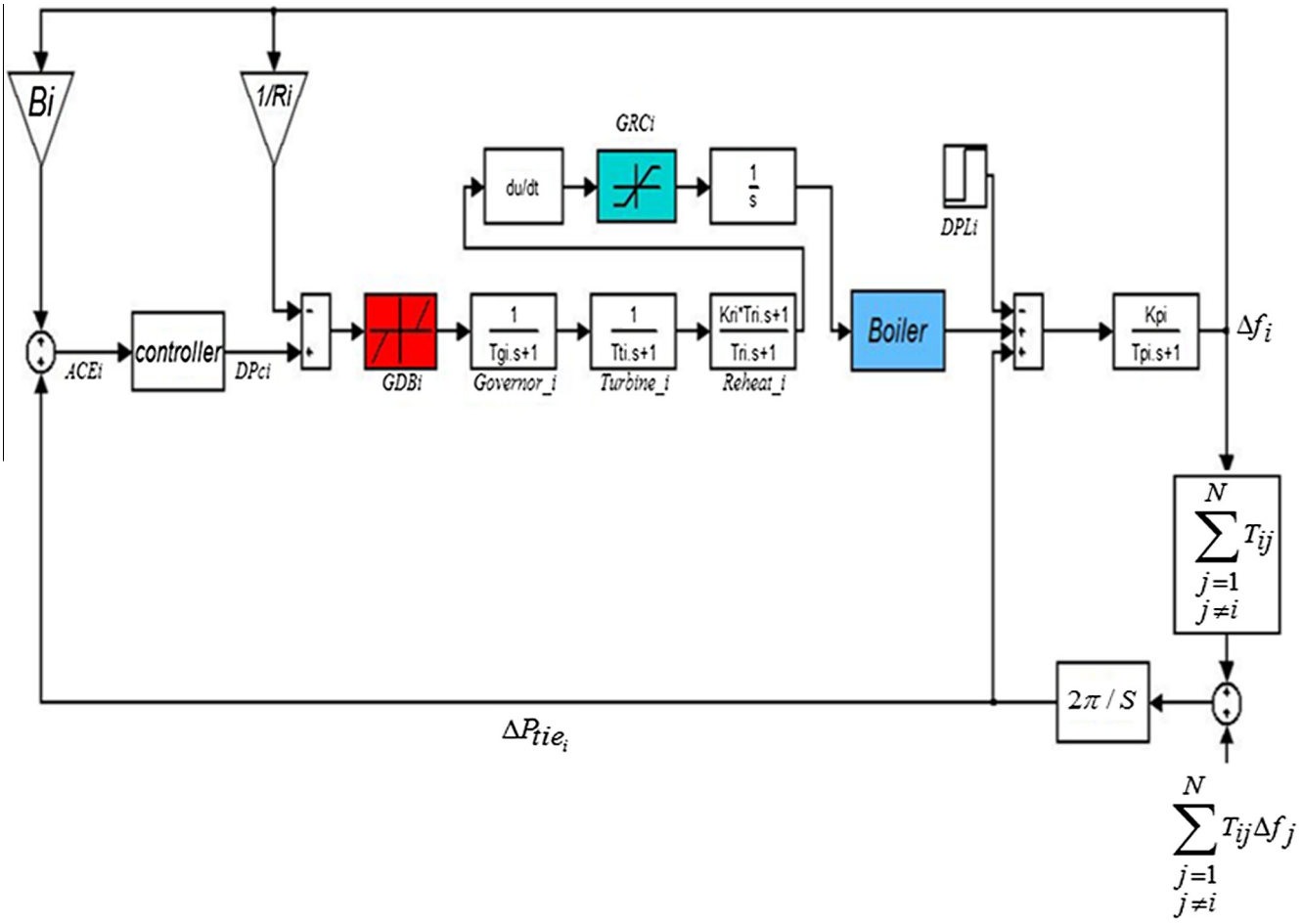

Figure 2 Transfer function model of the investigated system with nonlinearities.

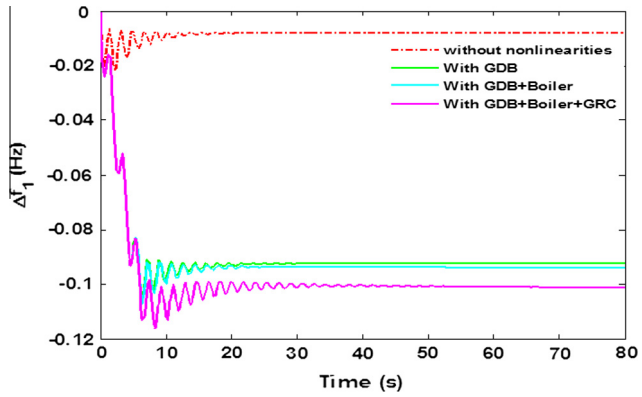

Figure 3 Dynamical frequency responses of the first area (Δf_1) with and without nonlinearities.

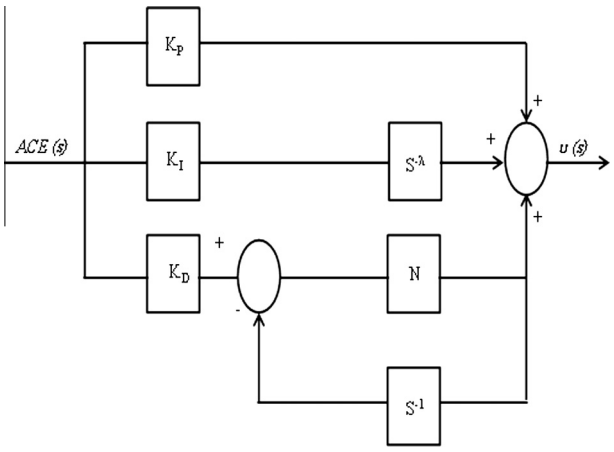

Figure 4 Investigated controller scheme.

$$\alpha = (\omega_h/\omega_l)^{v/n} \tag{6}$$

$$\eta = (\omega_h/\omega_l)^{1-v/N} \tag{7}$$

$$\omega_{z1} = \omega_l\sqrt{\eta} \tag{8}$$

$$\omega_{pn} = \omega_{z,n-1}\alpha, \quad n = 1\ldots N \tag{9}$$

$$\omega_{zn} = \omega_{p,n-1}\eta, \quad n = 2\ldots N \tag{10}$$

In this paper, the frequency range is selected as $\omega_l = 0.001$ rad/s, $\omega_h = 40$ rad/s and the number of zeros and poles is taken $N = 3$.

4. Fractional PID controller

The fractional order FO-PID (or PI$^{\lambda}$D$^{\mu}$) controller can be presented by the following differential equation as:

$$u(t) = K_p e(t) + K_I D_t^{-\lambda} e(t) + K_D D_t^{\mu} e(t) \tag{11}$$

where $u(t)$ is the control signal and $e(t)$ is the error signal which is the Area Control Error (ACE) in our case. After applying the Laplace transform to Eq. (11) considering the zero initial conditions, the transfer function can be stated by Eq. (12) as follows:

$$G_c(s) = K_P + K_I S^{-\lambda} + K_D S^{\mu} \tag{12}$$

In order to reduce the calculation time, noise effects and system discrete nonlinearities influence. The fractional derivative action is set to a simple filtered derivative action ($\mu = 1$). The transfer function of the investigated controller is written by the following:

$$G_c(s) = K_P + K_I S^{-\lambda} + K_D \frac{SN}{S+N} \tag{13}$$

The transfer function of investigated controller and the plane representation of different types of integer and fractional order controllers are presented in Figs. 4 and 5 respectively.

5. Optimization problem

5.1. Fitness function

In our study, the Integral of the Squared Error (*ISE*) criterion is used as a performance index and is given below:

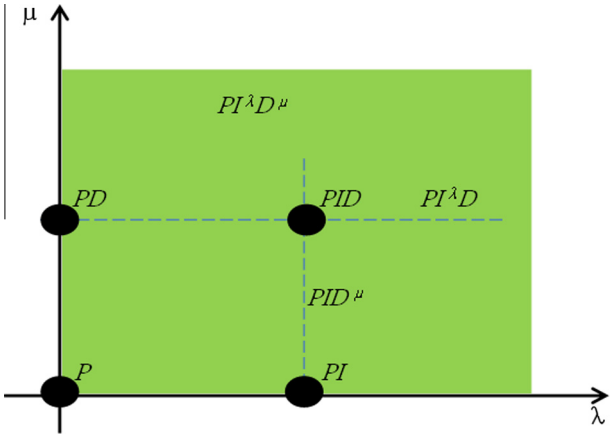

Figure 5 Plan representation of fractional PI$^{\lambda}$D$^{\mu}$ and classical PID controller.

$$J = ISE = \int_0^t \{ACE_1^2 + ACE_2^2 + ACE_3^2\}dt \tag{14}$$

In this case, the optimization problem can be formulated as follows:

$$\text{Minimize } J(K_P, K_I, K_D, \lambda, \mu \text{ and } N) \tag{15}$$

Subject to:

$$\begin{cases} K_p^{\min} \leqslant K_p \leqslant K_p^{\max} \\ K_I^{\min} \leqslant K_I \leqslant K_I^{\max} \\ K_D^{\min} \leqslant K_D \leqslant K_D^{\max} \\ \lambda^{\min} \leqslant \lambda \leqslant \lambda^{\max} \\ \mu^{\min} \leqslant \mu \leqslant \mu^{\max} \\ N^{\min} \leqslant N \leqslant N^{\max} \end{cases} \tag{16}$$

where K_P, K_I, K_D are the controller gains parameters, λ is an integral fraction, N is a derivative filter gain and the μ value is supposed equal to 1 as we have mentioned in the above section. The total number of parameters to be optimized in our case is equal to five for each area, four gains and one fraction. In this study, the bounded limits of gains have been fixed between 0 and 10. Fraction bounds were fixed between 0 and 1 and the derivative filter gain bounds were limited between 80 and 250.

Please cite this article in press as: Delassi A et al., Load frequency control problem in interconnected power systems using robust fractional PI$^{\lambda}$D controller, Ain Shams Eng J (2015), http://dx.doi.org/10.1016/j.asej.2015.10.004

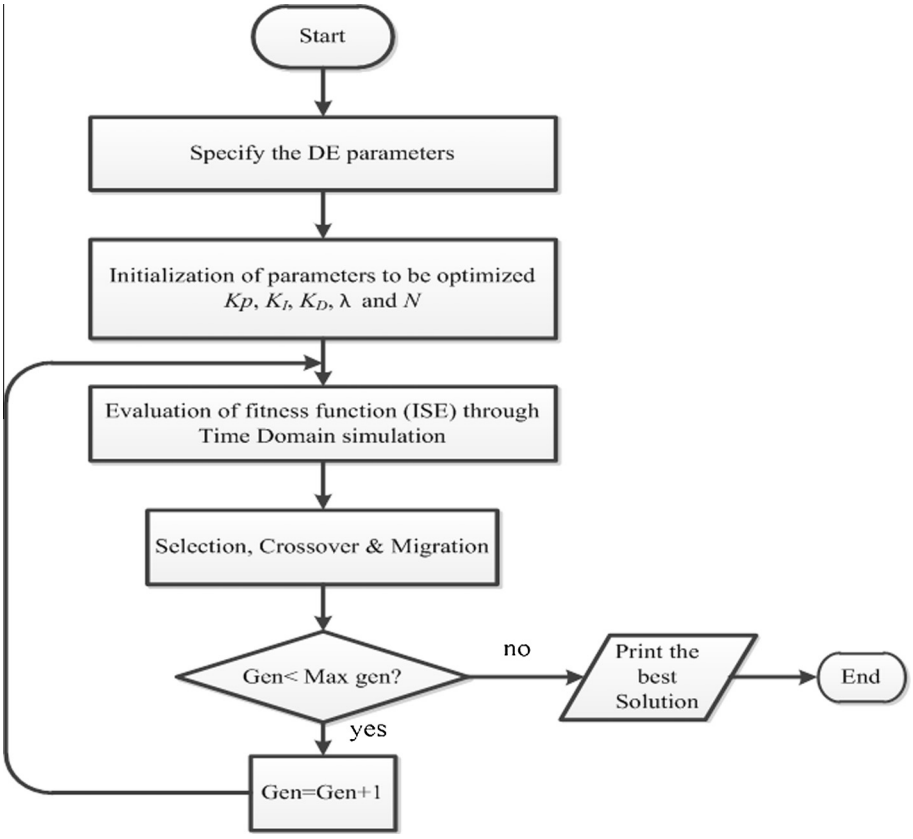

Figure 6 Flowchart of the optimal controller tuning using DE algorithm.

Table 1 DE settings.

Parameters	Value
Generations number	200
Population size	20
Crossover probability	0.8
Mutation probability	0.6

5.2. Differential Evolution Algorithm

The Differential Evolution Algorithm is a stochastic population-based optimization technique that belongs to the evolutionary algorithm class. It was introduced by Storn and Price in 1996. The DE algorithm can be used in such practical problem that is not even linear, noisy, continuous or has been many local minima. During the optimization process, this algorithm must spend by different steps resumed as follows [8,11,21,22]:

Table 2 Optimal controllers parameters given by the GA.

Controller parameters		K_P	K_I	K_D	N	Λ	μ
Area 1	PID	2.6061	2.9815	0.9249	233.9695	–	–
	$PI^{\lambda}D$	**2.4669**	**2.8993**	**0.8244**	**234.7685**	**0.8632**	**1**
	PID^{μ}	2.3465	3.1050	0.9522	–	–	0.9988
	$PI^{\lambda}D^{\mu}$	3.5206	3.0679	0.6562	–	0.8879	0.9999
Area2	PID	6.4217	1.4880	1.0348	249.2890	–	–
	$PI^{\lambda}D$	**4.9787**	**7.3753**	**3.2117**	**103.7146**	**0.6144**	**1**
	PID^{μ}	3.8931	1.1213	0.7173	–	–	0.999
	$PI^{\lambda}D^{\mu}$	5.0536	6.9426	3.5459	–	0.6753	0.9960
Area 3	PID	4.8397	1.1842	0.7462	190.5616	–	–
	$PI^{\lambda}D$	**3.5859**	**3.2101**	**1.7688**	**234.2188**	**0.7116**	**1**
	PID^{μ}	2.4469	0.5909	0.2195	–	–	0.9974
	$PI^{\lambda}D^{\mu}$	1.6750	8.3535	3.2371	–	0.5013	0.9948

Table 3 Optimal controllers parameters given by the DE algorithm.

Controller parameters		K_P	K_I	K_D	N	Λ	μ
Area 1	PID	9.8971	7.1301	1.9588	230.8075	–	–
	$PI^{\lambda}D$	**7.8272**	**8.9778**	**3.0474**	**228.1585**	**0.8496**	**1**
	PID^{μ}	8.3034	6.6277	1.7754	–	–	0.9894
	$PI^{\lambda}D^{\mu}$	0.8444	8.1509	2.5391	–	0.7633	0.9821
Area2	PID	8.1811	2.0674	1.4249	200.4645	–	–
	$PI^{\lambda}D$	**1.8754**	**9.8761**	**3.2276**	**208.0094**	**0.5153**	**1**
	PID^{μ}	9.5259	2.6097	1.4231	–	–	0.9934
	$PI^{\lambda}D^{\mu}$	2.2308	9.6725	3.2686	–	0.525	0.9839
Area 3	PID	9.7043	2.6573	1.7460	138.2870	–	–
	$PI^{\lambda}D$	**8.5179**	**9.8839**	**5.6325**	**125.5876**	**0.6593**	**1**
	PID^{μ}	8.1522	2.1004	1.0389	–	–	0.9839
	$PI^{\lambda}D^{\mu}$	5.3825	9.9178	4.6357	–	0.5909	0.9885

Table 4 Fitness value.

	GA		DE	
	ISE	C.P.U (mn)	ISE	C.P.U (mn)
PID	2.7202	43.0440	2.6810	47.0907
$PI^{\lambda}D$	**2.2409**	**61.1150**	**2.1348**	**64.8225**
PID^{μ}	2.87	59.4625	2.7695	61.5872
$PI^{\lambda}D^{\mu}$	2.2568	76.8870	2.1944	78.8602

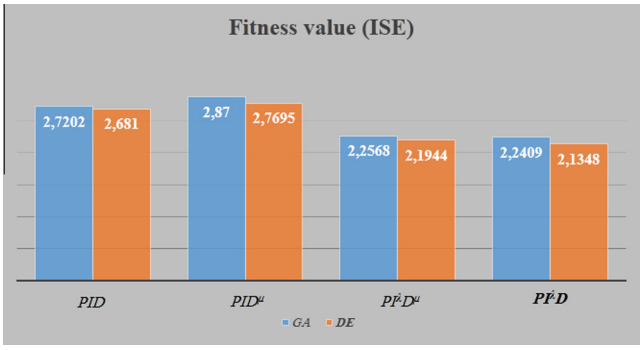

Figure 7 Diagram representation of fitness value using GA and DE algorithms for all controllers.

5.2.1. Initialization

For each parameter to be optimized the lower and upper bound must be defined. Then, an initial population will be randomly selected in this interval.

5.2.2. Migration

An initial mutant parameter vector, called donor vector $Vi, G + 1$ is created by choosing randomly three members of the population, $Xr1, G$, $Xr2, G$ and $Xr3, G$ such that the indices $i, r1, r2$ and $r3$ are distinct. The donor vector $Vi, G + 1$ written by Eq. (17) is created by adding a weighted difference between the two vectors in the third one.

$$V_{i,G+1} = X_{r1,G} + F(X_{r2,G} - X_{r3,G}) \tag{17}$$

where F is a mutation constant selected between (0, 2).

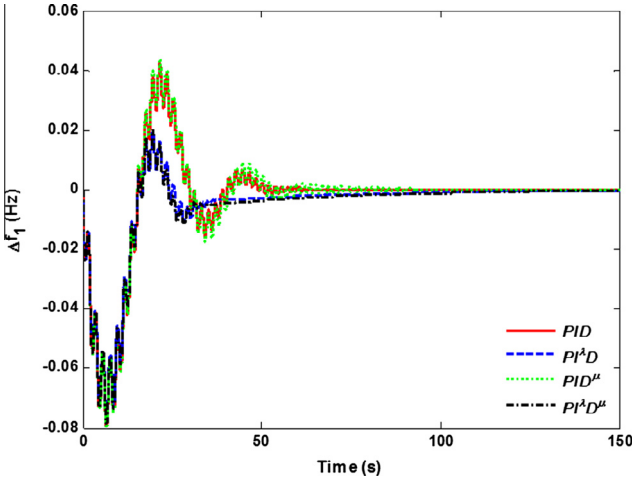

Figure 8a Dynamic response of Δf_1 according to 1% load disturbance in area 1 for different controllers.

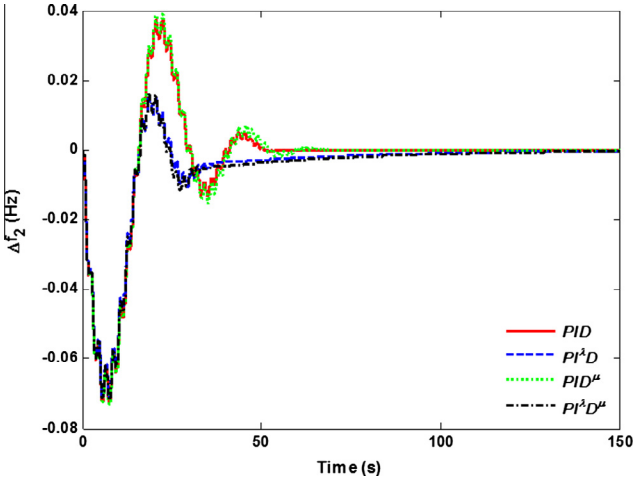

Figure 8b Dynamic response of Δf_2 according to 1% load disturbance in area 1 for different controllers.

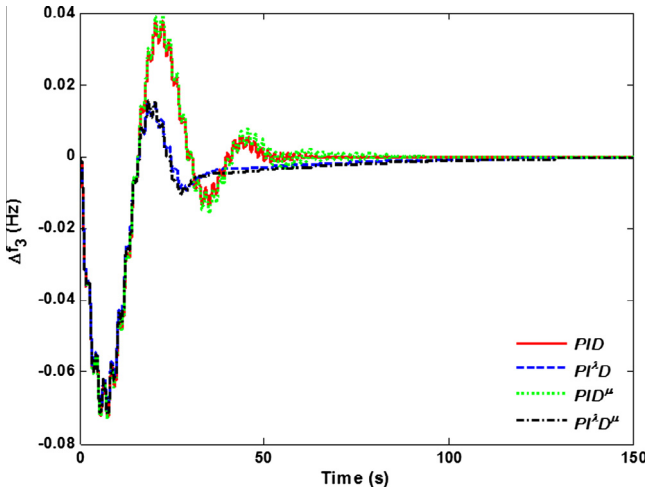

Figure 8c Dynamic response of Δf_3 according to 1% load disturbance in area 1 for different controllers.

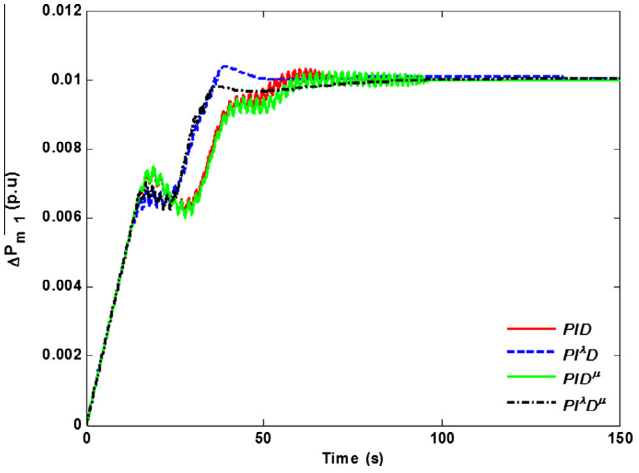

Figure 9a Dynamic response of $\Delta P_{tie_{12}}$ according to 1% load disturbance in area 1 for different controllers.

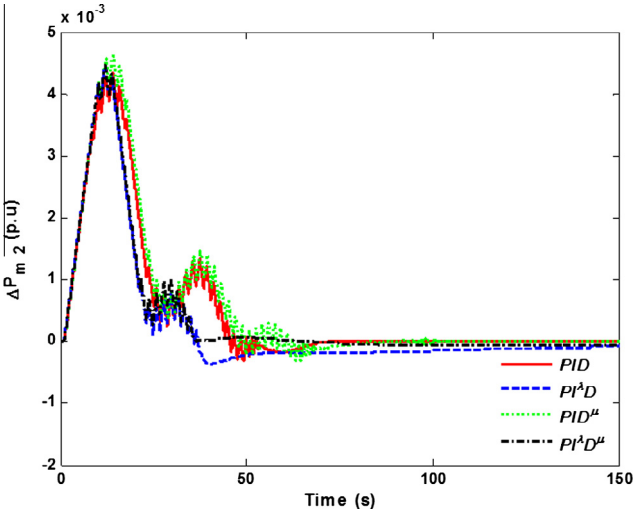

Figure 9b Dynamic response of $\Delta P_{tie_{13}}$ according to 1% load disturbance in area 1 for different controllers.

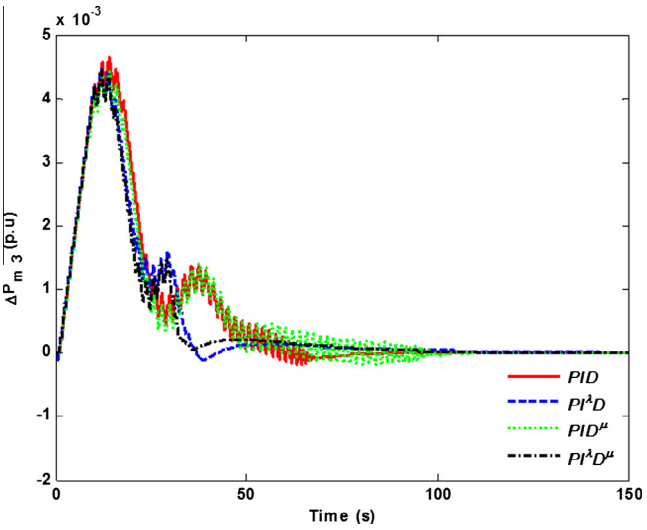

Figure 9c Dynamic response of $\Delta P_{tie_{23}}$ according to 1% load disturbance in area 1 for different controllers.

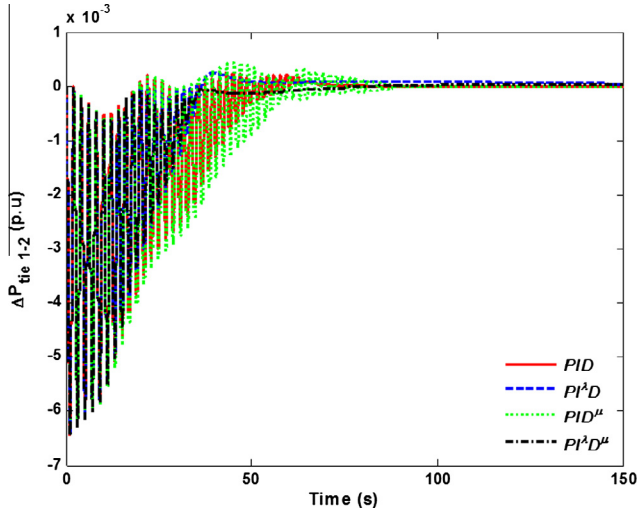

Figure 10a Dynamic response of ACE_1 according to 1% load disturbance in area 1 for different controllers.

5.2.3. Crossover

In order to improve the population potential diversity, a crossover operation is employed. In this phase, three parents are selected and the child is a perturbation of one of them. A trial vector $Ui,G + 1$ given by Eq. (18) is obtained from the target vector Xi, G, and the donor vector $Vi,G + 1$. The elements of the donor vector enter the trial vector with a probability of CR.

$$U_{j,i,G+1} = \begin{cases} V_{j,i,G+1} & \text{if } rand_{j,i} \leqslant CR \quad \text{or} \quad j = I_{\text{rand}} \\ X_{i,j,G} & \text{if } rand_{j,i} \succ CR \quad \text{and} \quad J \neq I_{\text{rand}} \end{cases} \quad i = 1, 2, \ldots, N; \quad j = 1, 2, \ldots, D \qquad (18)$$

5.2.4. Selection

In the selection step, the target vector $X_{i,G}$ is compared with the trial vector $V_{i,G+1}$ and the one which has the best fitness value is admitted to the next generation. The selection operator is given by Eq. (19).

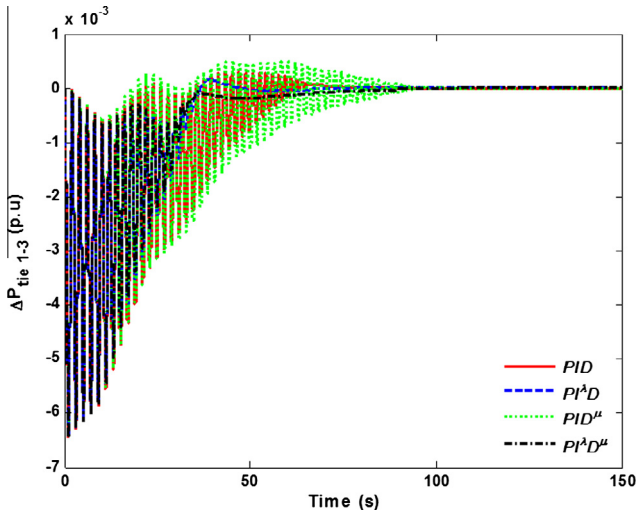

Figure 10b Dynamic response of ACE_2 according to 1% load disturbance in area 1 for different controllers.

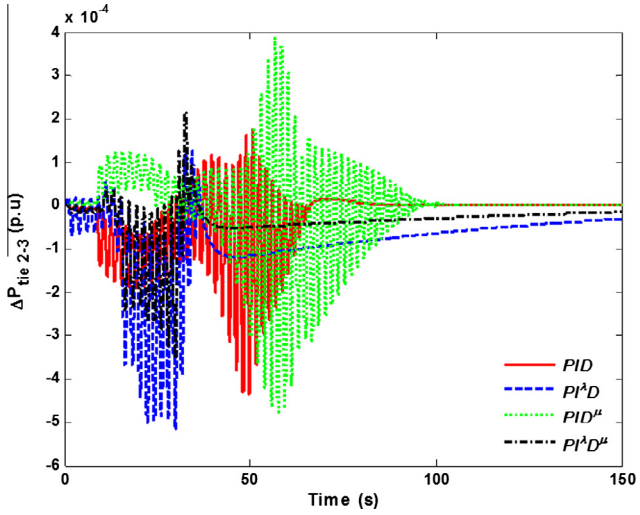

Figure 10c Dynamic response of ACE_3 according to 1% load disturbance in area 1 for different controllers.

$$X_{i,G+1} = \begin{cases} U_{i,G+1} & if\ f(U_{i,G+1}) \prec f(X_{i,G}) \\ X_{i,G} & \text{otherwise} \end{cases} \quad (19)$$

where $i \in [1, N_P]$.

DE algorithm process is repeated until some stopping criterion is reached. A general flowchart of the controller optimization procedure using the DE algorithm is depicted in Fig. 6. The DE algorithm settings are tabulated in Table 1.

6. Simulation results and discussion

To validate the efficiency of the investigated controller, simulations were carried out for three areas reheat-thermal system shown in Fig. 1. Then, three nonlinear constraints (*GDB*, *GRC* and dynamic boiler) are taken into consideration. According to 1% load disturbance in area 1 (ΔP_{L1} = 1% p.u), the DE

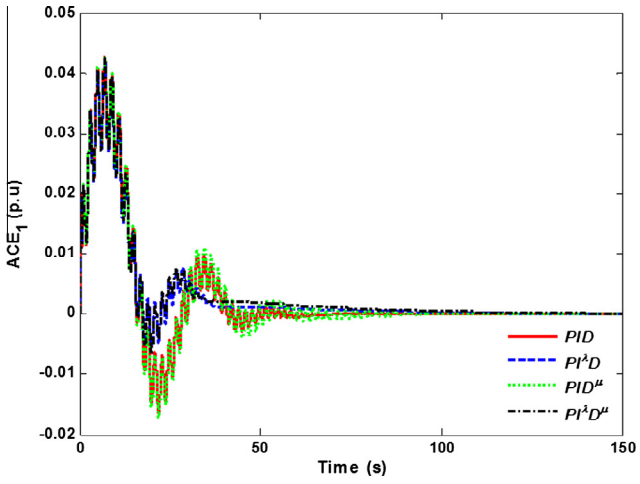

Figure 11a Dynamic response of ΔP_{m_1} according to 1% load disturbance in area 1 for different controllers.

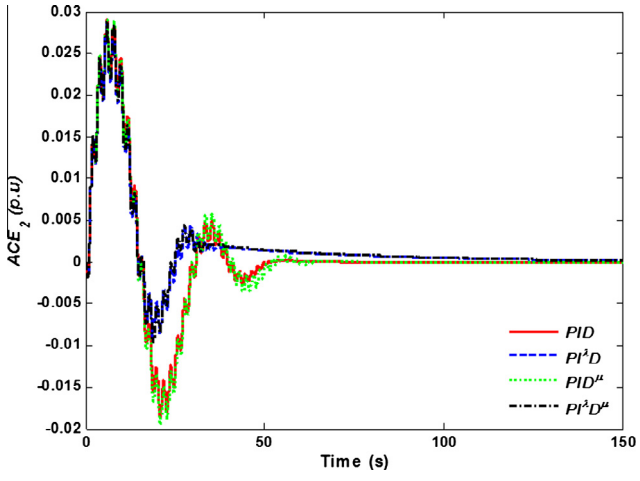

Figure 11b Dynamic response of ΔP_{m_2} according to 1% load disturbance in area 1 for different controllers.

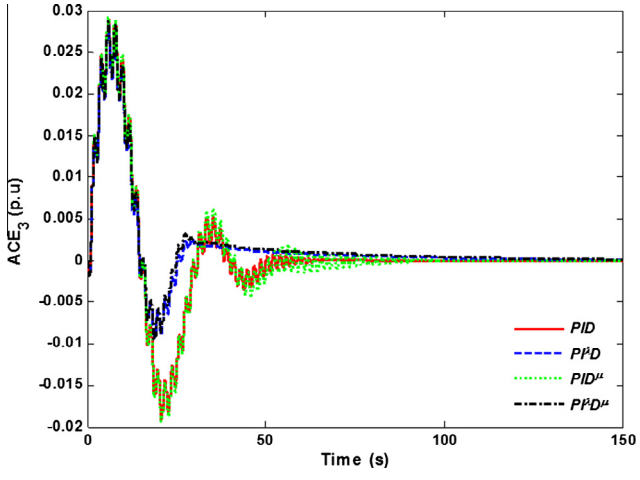

Figure 11c Dynamic response of ΔP_{m_3} according to 1% load disturbance in area 1 for different controllers.

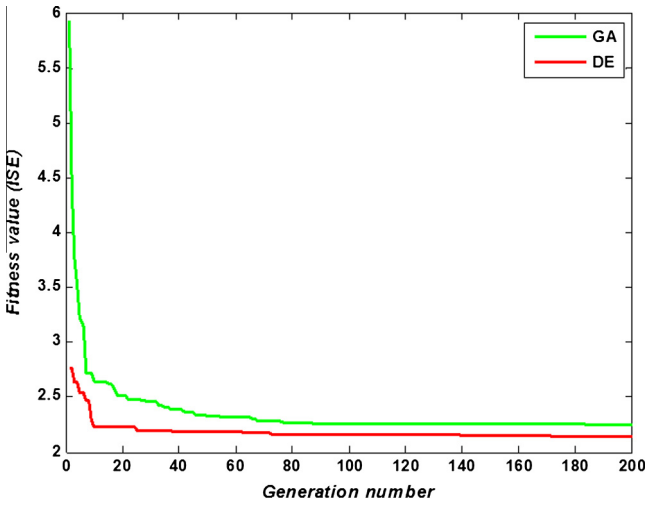

Figure 12 Fitness function (*ISE*) evaluation with GA and DE algorithms.

algorithm is executed to find the optimal controllers parameters, using the *ISE* criterion as a performance index. The effectiveness of the investigated controller is compared with classical filtered PID, PID$^{\mu}$ and PI$^{\lambda}$D$^{\mu}$. The effectiveness of the DE algorithm is compared to the GA. The same system parameters and DE settings are used for each controller to make a fair comparison. After the optimization process, the optimal settings of the investigated controller and the other controllers as well as the performance index and C.P.U time are presented in Tables 2–4 simultaneously. Diagram representation of fitness value using GA and DE algorithms for all controllers is displayed in Fig. 7. All areas dynamic response of frequency deviation, tie line power deviation, Area control error and mechanical power deviation are displayed in Figs. 8a–8c, 9a–9c, 10a–10c and 11a–11c respectively.

The Peak Overshoot (P.O), the Peak Undershoot (P.U) and the settling time (S.T) of Figs. 8a–8c, 9a–9c, 10a–10c and 11a–11c corresponding to the proposed **PI$^{\lambda}$D**, simple PID, PID$^{\mu}$ and PI$^{\lambda}$D$^{\mu}$ controllers are tabulated in Tables 5 and 6 respectively.

From these results, it is observed that the *ISE* criterion corresponding to the proposed (**PI$^{\lambda}$D**) controller is decreased by 20.37% compared to the classical PID controller in the case of the DE algorithm and by 17.62% in the case of the GA. It is clearly remarked that the proposed controller has better performance compared to the classical PID in terms of peak overshoots, peak undershoots and settling time. Also, the proposed controller is compared to the fractional controllers such as PID$^{\mu}$ and PI$^{\lambda}$D$^{\mu}$ in order to show the rapidity and the efficiency of the proposed **PI$^{\lambda}$D** controller, and it is noted that our controller reduces the calculation time by 17.8% compared to the PI$^{\lambda}$D$^{\mu}$ controller and the performance index by 22.91% compared to the PID$^{\mu}$ controller. Elsewhere, Fig. 12 presents a comparison between the GA and the DE algorithm in terms of convergence rapidity. From this figure, the superiority of DE algorithm compared to the GA is clearly revealed. From Tables 5 and 6, all areas frequency deviation (Δf_1, Δf_2 and Δf_3) emphasizes that the system is clearly stable with all controllers, which is the frequency margin (maximum and minimum deviation Δf_i) considered in the practice equal to ± 0.5 Hz from its nominal value. The maximum and minimum deviations for all controllers (PID, **PI$^{\lambda}$D**, PID$^{\mu}$ and PI$^{\lambda}$D$^{\mu}$) respect this limits.

6.1. Robustness analysis

In order to show the robustness of the proposed **PI$^{\lambda}$D** controller, two tests (scenarios *a* and *b*) corresponding to a high

Table 5 Dynamic performance of the PID and the PI$^{\lambda}$D controllers.

Dynamic response	*P.O*		*P.U*		*S.T*	
	PID	*PI$^{\lambda}$D*	*PID*	*PI$^{\lambda}$D*	*PID*	*PI$^{\lambda}$D*
Δf_1	0.0424	0.0198	−0.079	−0.0777	50.3595	49.1489
Δf_2	0.0377	0.0158	−0.0726	−0.0712	49.0295	51.0051
Δf_3	0.0377	0.0152	−0.0726	−0.0710	53.8171	51.0841
ΔP_{TIE12}	0.000265	0.000247	−0.0035	0.0000683	62.6815	41.9520
ΔP_{m1}	0.0103	0.014	0.0088	0.009	65.56668	42.3287
ACE_1	0.0098	0.042	−0.0164	−0.063	53.333	37.1838

Table 6 Dynamic performance of the PID$^{\mu}$ and the PI$^{\lambda}$D$^{\mu}$ controllers.

Dynamic response	*P.O*		*P.U*		*S.T*	
	PID$^{\mu}$	*PI$^{\lambda}$D$^{\mu}$*	*PID$^{\mu}$*	*PI$^{\lambda}$D$^{\mu}$*	*PID$^{\mu}$*	*PI$^{\lambda}$D$^{\mu}$*
Δf_1	0.0441	0.02	−0.0795	−0.0784	77.6367	54.0942
Δf_2	0.0392	0.0162	−0.0153	−0.0719	57.2392	55.7974
Δf_3	0.0394	0.0157	−0.0156	−0.0719	79.3467	55.8073
ΔP_{TIE12}	0.000434	−0.0000064	−0.0037	−0.0064	78.9868	35.2114
ΔP_{m1}	0.0102	0.0099	0.009	0.0087	78.8485	57.1687
ACE_1	0.0428	0.0423	−0.0171	−0.064	74.3976	55.1461

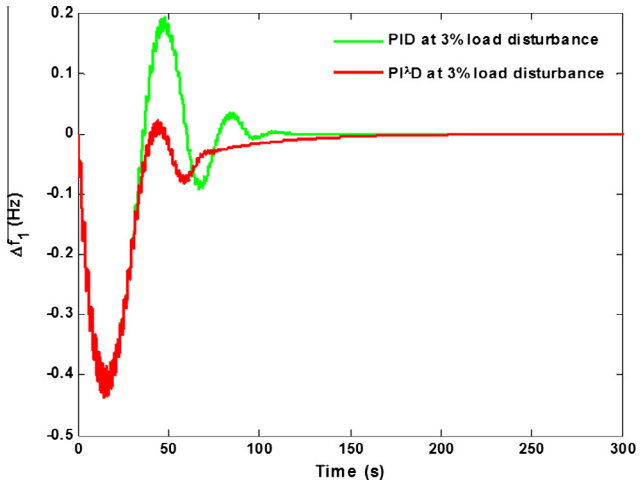

Figure 13a Dynamic response of Δf_1 in area 1 according to 3% load disturbance.

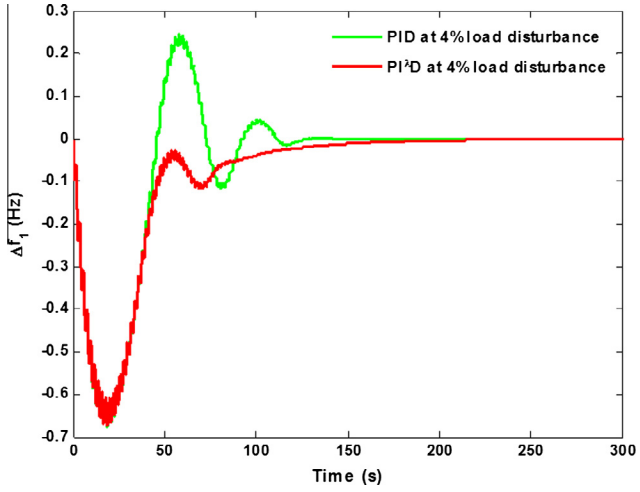

Figure 13b Dynamic response of Δf_1 in area 1 according to 4% load disturbance.

load disturbance and severe parametric variations (sensitivity analysis) have been applied. The same controller parameters obtained above are used in this section.

6.1.1. Load disturbance

For this scenario, a 3% and 4% load disturbance in area one is applied. Figs. 13a and 13b show the frequency deviation in area 1 according to these load disturbances respectively.

6.1.2. Sensitivity analysis

For this scenario, the turbine governor time constant (T_{Gi}), the turbine time constant (T_{Ti}) and the tie line time constant (T_{ij}) are modified progressively from −50% to +50% respect with a step of 25%. The dynamic response, of Δf_1 for all those cases is presented in Figs. 14–16 simultaneously. The peak overshoots, peak undershoots, settling time and the performance index (*ISE*) of those responses are presented in Table 7.

From these results, it is obvious that the investigated controller is high-performing in terms of the effectiveness and

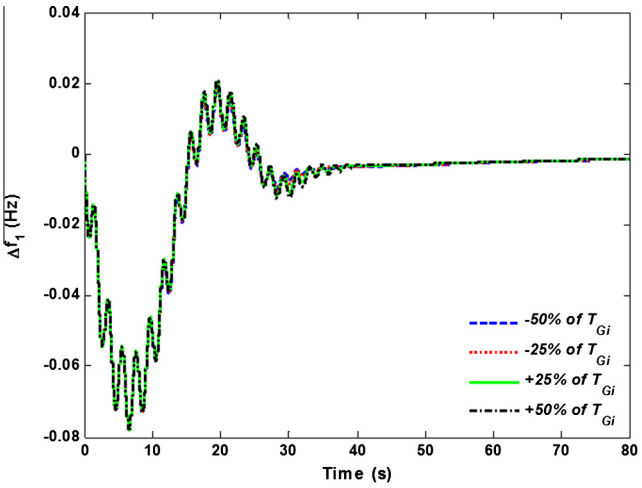

Figure 14 Dynamic response of Δf_1, according to a 1% change in area 1 with varying the turbine governor time constant.

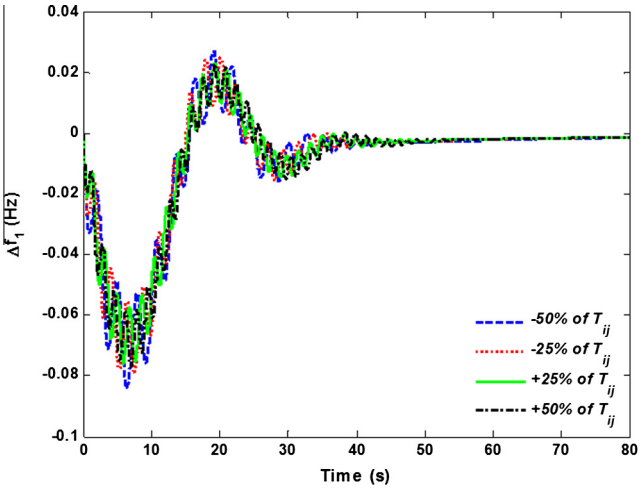

Figure 15 Dynamic response of Δf_1, according to a 1% change in area 1 with varying the turbine time constant.

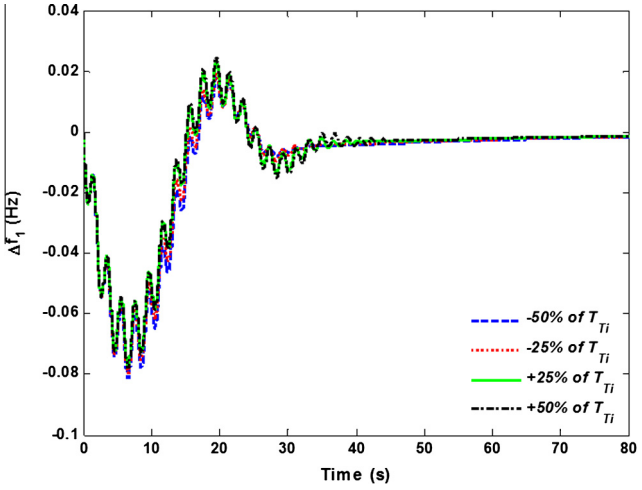

Figure 16 Dynamic response of Δf_1, according to a 1% change in area 1 with varying the tie-line time constant.

Table 7 Sensitivity analysis.

Dynamic response	*P.O*		*P.U*		*ST*		*ISE*
	Δf_1	Δf_2	Δf_1	Δf_2	Δf_1	Δf_2	
Nominal	0.0198	0.0158	−0.0777	−0.0712	49.1489	51.0051	2.1348
−50% T_{Gi}	0.0188	0.015	−0.0781	−0.0718	50.1184	51.8507	2.1616
−25% T_{Gi}	0.0193	0.0154	−0.0780	−0.0717	49.6998	51.4677	2.1593
+25% T_{Gi}	0.0204	0.0163	−0.0779	−0.0715	48.5434	51.4867	2.1562
+50% T_{Gi}	0.0211	0.0169	−0.0781	−0.0717	47.5091	49.7647	2.1811
−50% T_{Ti}	0.0177	0.0156	−0.0815	−0.0761	51.9089	53.2634	2.4778
−25% T_{Ti}	0.0192	0.0161	−0.0798	−0.0739	50.5544	52.1073	2.3246
+25% T_{Ti}	0.0229	0.0185	−0.0770	−0.0716	47.3553	49.5715	2.1783
+50% T_{Ti}	0.0243	0.0197	−0.0783	−0.0719	45.1843	47.6497	2.2073
− 50% T_{ij}	0.0247	0.0185	−0.0841	−0.0751	48.9077	51.1897	2.3040
−25% T_{ij}	0.0224	0.0191	−0.0792	−0.0741	48.6399	49.9403	2.2172
+25% T_{ij}	0.0202	0.0181	−0.0790	−0.0754	49.7335	50.6554	2.4265
+50% T_{ij}	0.0209	0.0182	−0.0806	−0.0758	49.0234	50.5070	2.5768

the robustness against higher degree of load disturbance and severe parametric variation from different point of views. In fact, in all cases, the overshoot, undershoot, settling time and index performance changes did not exceed 19.79%, 7.60%, 5.31% and 17.15% respectively.

7. Conclusion

This paper presents the design of a robust fractional **PI$^{\lambda}$D** controller, made up with a fractional integral action and a simple filtered derivative action. Firstly, the proposed controller has been applied to an AGC of a three area reheat-thermal systems considering several nonlinear constraints such as GDB, GRC and boiler dynamics. The optimal controller parameters have been tuned through an evolutionary algorithm called Differential Evolution Algorithm. The Integral of Squared Error is chosen as a performance index. Then, the performance of a classical PID controller, PID$^{\mu}$ and PI$^{\lambda}$D$^{\mu}$ is studied and its corresponding dynamic responses were compared to the proposed controller. Finally, the robustness analysis of the proposed controller against higher degree of load disturbance and severe parametric variations reveals that this controller performed well compared to the other controllers from different point of views.

Appendix A. The nominal system parameters under study are given below

$f = 60$ Hz, $T_{Gi} = 0.08$ s, $T_{ri} = 10$ s, $2Hi = 0.1666$ s, $T_{Ti} = 0.3$ s, $K_r = 0.5$, $D_i = 0.00833$ p.u MW/Hz, $T_{pi} = 20$ s, $K_{pi} = 120$ Hz/p.u MW, Initial loading = 50%, $T_{ij} = 0.086$.

A.1. Boiler dynamics

$K_1 = 0.85$, $K_2 = 0.095$, $K_3 = 0.92$; $T_d = 0$, $T_f = 10$, $C_B = 200$, $K_{IB} = 0.03$, $T_{IB} = 26$, $T_{RB} = 69$.

A.2. Nonlinearities

In this study, the GDB and GRC limits taken into account are given below:

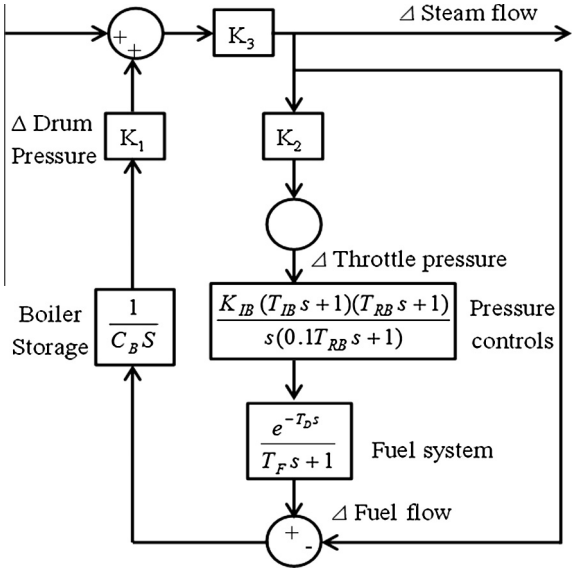

Figure B1 Dynamic boiler scheme.

GDB = ± 0.036 Hz and GRC = ± 3% per minutes = 0.0005 p.u MW/min

Appendix B

See Fig. B1.

References

[1] Shayeghi H, Shayanfar HA, Jalili A. Load frequency control strategies: a state-of-the-art survey for the researcher. Energy Convers Manage 2009;50:344–53.
[2] Khodabakhshian A, Ezatabadi Pour M, Hooshmand R. Design of a robust load frequency control using sequential quadratic programming technique. Electr Power Energy Syst 2012;40:1–8.
[3] Sudha KR, Vijaya Santhi R. Load frequency control of an interconnected reheat thermal system using type-2 fuzzy system including SMES units. Electr Power Energy Syst 2012;43:1383–92.
[4] Wood Allen J, Wollenberg Bruce F. Power generation operation and control; 1996.

[5] Kundur P. Power system stability and control. 5th reprint. New Delhi: Tata McGraw-Hill; 1994.
[6] Saadat H. Power system analysis. USA: McGraw-Hill; 1999.
[7] Bevrani H. Robust power system frequency control. Springer; 2009.
[8] Umesh KR, Rabindra KS, Sidhartha P. Design and analysis of differential evolution algorithm based automatic generation control for interconnected power system. Ain Shams Eng J 2013;4:409–21.
[9] Abdel-Magid YL, Dawoud MM. Optimal AGC tuning with genetic algorithms. Electr Power Syst Res 1997;38:231–8.
[10] Sidhartha P, Banaja M, Hota PK. Hybrid BFOA–PSO algorithm for automatic generation control of linear and nonlinear interconnected power systems. Appl Soft Comput 2013;13: 4718–30.
[11] Rabindra KS, Sidhartha P, Umesh KR. DE optimized parallel 2-DOF PID controller for load frequency control of power system with governor dead-band nonlinearity. Electr Power Energy Syst 2013;49:19–33.
[12] Subha S. Load frequency control with fuzzy logic controller considering governor dead band and generation rate constraint nonlinearities. World Appl Sci J 2014;29:1059–66.
[13] Muwaffaq IA. Load frequency control and automatic generation control using fractional-order controllers. Electr Eng 2010;91: 357–68.
[14] Sanjoy D, Lalit CS, Nidul S. AGC of a multi-area thermal system under deregulated environment using a non-integer controller. Electr Power Syst Res 2013;95:175–83.
[15] Ramakrishna KSS, Sharma P, Bhatti TS. Automatic generation control of interconnected power system with diverse sources of power generation. Int J Eng Sci Technol 2010;2:51–65.
[16] Kanendra N, Hazlie M. Application of firefly algorithm with online wavelet filter in automatic generation control of an interconnected reheat thermal power system. Electr Power Energy Syst 2014;63:401–13.
[17] Sanjoy D, Lalit CS, Nidul S. Solution to automatic generation control problem using firefly algorithm optimized $I^{\lambda}D^{\mu}$ controller. ISA Trans 2014;53:358–66.
[18] Sanjoy D, Lalit CS, Nidul S. Automatic generation control using two degree of freedom fractional order PID controller. Electr Power Energy Syst 2014;58:120–9.
[19] Sanjoy D. Robust two-degree-of-freedom controller for automatic generation control of multi-area system. Electr Power Energy Syst 2014;63:878–86.
[20] Sayed AT, Masoud HF, Saber FA. Fractional order PID controller design for LFC in electric power systems using imperialist competitive algorithm. Ain Shams Eng J 2014;5: 121–35.
[21] Duarte Pedro Mata de Oliveira Valério. Ninteger v. 2.3 Fractional control toolbox for MatLab.
[22] Banaja M, Sidhartha P, Hota PK. Differential evolution algorithm based automatic generation control for interconnected power systems with nonlinearity. Alexandria Eng J 2014;53: 537–52.

Abdelmoumène Delassi was born in Laghouat, Algeria, in 1990. He obtained his License and Master degrees from Electrical engineering department, Laghouat University in 2011 and 2013 respectively. He is toward working in his Ph.D thesis on Electrical Power System. He is also a Member in LACoSERE Laboratory. His current research interests include Power system stability and control, optimization techniques and Artificial intelligence.

Salem Arif was born in Taibat, Ouargla, Algeria, in 1968. He obtained his Electrical Engineering diploma in 1992, his Magister and Ph.D degrees in Electrical Power System at Polytechnic National School of Algiers, Algeria, in 1995 and 2008 respectively.
In 1998, he joined the Electrical Engineering Department, Laghouat University, Algeria, as an Assistant Lecturer. Since March 2010, he is an Assistant Professor at the same Department. He is also a Team Leader of "Power System Optimization and Control" research group of LACoSERE Laboratory, Laghouat University, Algeria. His research interests include, planning and optimization problems in Electrical power systems, reactive power static compensators, Optimization techniques.

Lakhdar Mokrani was born in Batna, Algeria, in 1970. He obtained his engineer and Ph.D. degrees in electrical engineering, in 1994 and 2005 respectively from Batna University, Algeria.
In 1997, he joined the Electrical Engineering Department of Laghouat University, Algeria, as Assistant Lecturer. Since December 2005, he is an Assistant Professor at the same department. He is also a Team Leader of "Control and Energy Management of Electrical Systems" research group in the LACoSERE laboratory, Laghouat University, Algeria. Since 2012, he is a Professor at the same Department. His main research area includes Modeling and CAD of Electrical Machines, Electrical Drives Control and Renewable Energy Systems Control and Management.

Please cite this article in press as: Delassi A et al., Load frequency control problem in interconnected power systems using robust fractional $PI^{\lambda}D$ controller, Ain Shams Eng J (2015), http://dx.doi.org/10.1016/j.asej.2015.10.004